

1 **LEPY: A Python-Based Pipeline for Automated**

2 **Morphological Trait Analysis of Lepidoptera Images**

3

4 Yenny Correa-Carmona^{1,2}, Dennis Böttger¹, Dimitri Korsch³, Kim L. Holzmann⁴, Pedro Alonso-
5 Alonso⁴, Andrea Pinos⁵, Felipe Yon^{6,7}, Alexander Keller⁵, Ingolf Steffan-Dewenter⁴, Marcell K.
6 Peters⁴ and Gunnar Brehm¹

7

8 ¹ Institut für Zoologie und Evolutionsbiologie mit Phyletischem Museum, Friedrich-Schiller University
9 Jena, 07743 Jena, Germany

10 ² Grupo de Entomología Universidad de Antioquia (GEUA), Universidad de Antioquia, Medellín,
11 Colombia

12 ³ Thüringer Zentrum für Lernende Systeme und Robotik (TZLR), Technische Universität Ilmenau, 98693
13 Ilmenau

14 ⁴ Department of Animal Ecology and Tropical Biology, Biocenter, University of Würzburg, 97074
15 Würzburg, Germany

16 ⁵ Cellular and Organismic Networks, Faculty of Biology, Ludwig-Maximilians University Munich, 82152
17 Planegg-Martinsried, Germany

18 ⁶ Departamento de Ciencias Biológicas y Fisiológicas, Facultad de Ciencias e Ingeniería, Universidad
19 Peruana Cayetano Heredia, 15102 Lima, Peru

20 ⁷ Instituto de Medicina Tropical, Universidad Peruana Cayetano Heredia, 15102 Lima, Peru

21 **Correspondence**

22 Yenny Correa-Carmona

23 Email: yennycorreacarmona@gmail.com

24 **Funding information**

25 The Research Unit ANDIV (<https://www.andiv.biozentrum.uni-wuerzburg.de/>);

26 Deutsche Forschungsgemeinschaft (DFG) under grants PE 1781/4-1, BR 2280/9-1, STE 957/29-1
27 and KE 1743/12-1.

28 TZLR project is founded by Thuringian Ministry of Economics, Science and Digital Society (2023 - 2025).

29 **Abstract**

30 1. We present LEPY, a Python-based pipeline for automating the extraction and analysis of
31 morphological traits, including structural and colour properties, from mounted Lepidoptera
32 specimens. It uses a U-Net neural network for image segmentation and a scale bar for precise
33 measurements. LEPY is designed to be easy and reproducible, ensuring efficient and
34 consistent analysis of large Lepidoptera image datasets. It also supports the integration of UV
35 photographs for enhanced colour analysis.

36 2. LEPY computes structural traits, including body and wing length and area, and colour
37 characteristics such as hue, saturation, and intensity, which are stored in a structured format
38 (CSV) for easy evaluation. It also provides distribution metrics that describe the brightness and
39 dynamic range/contrast, chromaticity, and luminance for four colour channels (R, G, B, and
40 UV). Data from all channels are integrated to calculate colour diversity using the Shannon
41 index. A visual summary of each image pair, including false colour images, is also provided.

42 3. We validated LEPY using data from Sphingidae and Saturniidae moths, known for their
43 contrasting traits, which were sampled along a complete elevational gradient in the Peruvian
44 Andes. In both families, forewing length increased with elevation. As expected, Sphingidae
45 had smaller wing areas than Saturniidae despite their longer forewings. The brightness of
46 colours decreased with elevation in both families, and Sphingidae were generally darker than
47 Saturniidae. The dynamic range/contrast varied among species but was uncorrelated to
48 elevation.

49 4. LEPY is a powerful tool for studying key Lepidoptera traits. It integrates advanced computer
50 vision and neural network methods to automated measurements, supporting ecological and

51 evolutionary research. It also offers new possibilities for analysing Lepidoptera traits along
52 gradients and responses to environmental changes.

53 **KEYWORDS**

54 Computer Vision, Deep Learning, Lepidoptera, Multispectral Colour Analysis, Structural Traits,
55 Python, Photography, UV Photography

56

57 **1 | INTRODUCTION**

58 Integrating measures of functional traits of organisms and their change with environmental
59 stressors is becoming increasingly important in ecological research (Correa-Carmona et al.,
60 2022; Gámez-Virués et al., 2015; Wellstein et al., 2011). This can be particularly challenging
61 in insects which are the most diverse and abundant organisms on Earth, and it is usually very
62 time-consuming to identify, prepare and measure their morphological traits (van Klink et al.,
63 2022). Lepidoptera – butterflies and moths – is one of the most diverse insect clades, are no
64 exception with this regard (Freitas et al., 2020). They have been used as a model group for
65 many studies in ecology and evolution (Watt & Boggs, 2003; Hill et al., 2021), because at least
66 the largest and most conspicuous groups have traditionally been intensively collected.
67 Lepidopteran taxonomy is on average better studied than in other insect orders, with notable
68 exceptions in which more difficult molecular analysis or other tools for identification are
69 required (Lamarre et al., 2022; Moraes et al., 2021; Murillo-Ramos et al., 2021).

70

71 Body size is probably the most important and the most studied functional trait, as it is linked to
72 population vital rates (metabolism, survival, growth, reproduction) and to ecological
73 interactions (Brehm et al., 2019; Woodward et al., 2005). It is also one of the most sensitive
74 traits to environmental change (Chown & Gaston, 2010; Cortés-Gómez et al., 2023; Tammaru
75 & Teder, 2012). Another important morphological trait of insects is their colouration. Colour is

76 particularly important in Lepidoptera, because it is used for a variety of purposes, such as body
77 protection (i.e., camouflage, mimicry), signalling and physiological/thermal adaptation
78 (Heidrich et al., 2018; Koičková et al., 2012). Wing colour patterns are also of key importance
79 for species-level identification (Feng et al., 2015). The UV (ultraviolet) colouration of
80 Lepidoptera is also of vital importance in a wide range of biological and ecological contexts
81 (Brehm et al., 2021; Heidrich et al., 2018; Koičková et al., 2012). UV patterns, invisible to
82 mammals including humans, but perceptible to a wide range of other organisms (e.g., most
83 arthropods and birds), play an important role in communication (Cronin & Bok, 2016; Paul &
84 Gwynn-Jones, 2003). For example, visual signals can attract mates or to distinguish
85 conspecifics from other species (Bálint et al., 2012), they are important for survival (camouflage
86 or mimicry strategies; Lyytinen et al., 2004; Zapletalová et al., 2016) and evolutionary
87 processes (e.g., pollination; Ohashi et al., 2015; Papiorek et al., 2016). However, relatively few
88 studies have been carried out that include UV patterns of insects in general and of Lepidoptera
89 in particular (Stella & Kleisner, 2022), and digitisation programmes in biological collections
90 have usually neglected UV patterns (Brehm, 2025).

91

92 Traditional manual methods for measuring morphological traits in entomology are usually time
93 consuming and prone to human error (Fountain-Jones et al., 2015). In the case of Lepidoptera,
94 wing structures are also delicate and can be easily damaged. Recently, several studies
95 investigated ways to automate the detection, classification, and measurement of functional
96 traits such as wing and body size, coloration, and coloration patterns in Lepidoptera by using
97 modern approaches such as computer vision and machine learning, offering ways to save time
98 and improve the accuracy of these measurements (Feng et al., 2015; Høye et al., 2021;
99 Manoukis & Collier, 2019; Palma et al., 2023). Computer vision and deep learning techniques
100 have significantly advanced the field of entomology by reducing reliance on manual
101 measurements, enabling large-scale, high-throughput analyses, and improving the accuracy
102 and reproducibility of trait measurements (Høye et al., 2021; Manoukis & Collier, 2019; Palma
103 et al., 2023). Python is the most used programming language for developing these techniques

104 (Van Rossum & Drake, 2009), thanks to its advanced image analysis frameworks,
105 comprehensive and extensive scientific libraries/tools, broad user community, and continuous
106 contributions from third-party developers, ensuring its adaptability for new applications.
107 Pipelines already exist in the field of automated analysis of Lepidopteran images, including
108 MothSeg and Mothra. MothSeg (<https://github.com/erodner/mothseg>) contains Python-based
109 tools for segmenting and analysing images of moths and butterflies in dorsal and ventral
110 position using a scale. Mothseg provides mean, median, and standard deviation of hue,
111 saturation, and intensity of an RGB image, and calculates the width of the moth shape as well
112 as the area of body + wings (Jaimes Nino et al., 2019). However, options for body size
113 measurements are limited, and it takes 3 to 5 minutes to analyse a single image. Another
114 computer vision pipeline is Mothra (Wilson et al., 2023); it automatically detects the specimen
115 and other objects in the image, adjusts the scale, measures wing characteristics (e.g., forewing
116 length), determines the orientation of the image (vertical or horizontal), and identifies sex by
117 assessing patterns of sexual size dimorphism. Mothra is also limited regarding the number of
118 morphological traits and does not analyse colours.

119

120 In this paper we introduce LEPY, a Python-based tool for the automatic segmentation and
121 analysis of lepidopteran structural and colour traits. Our goal was to integrate key features from
122 existing algorithms with significant new features, especially in quantitative colour analysis,
123 including information on UV reflectance. We aimed to enhance segmentation accuracy through
124 deep learning models and incorporate a configurable calibration step to extract comprehensive
125 measurements more efficiently. We also wanted to develop a structured trait data to store all
126 trait data and a visualization system that highlights key morphological traits alongside density
127 plots of colour channels. To validate LEPY's utility, we applied it to a dataset of two well-studied
128 moth families, viz. Sphingidae and Saturniidae, collected along an elevational gradient in Peru.

129 2 | MATERIALS AND METHODS

130 2.1 | Implementation details

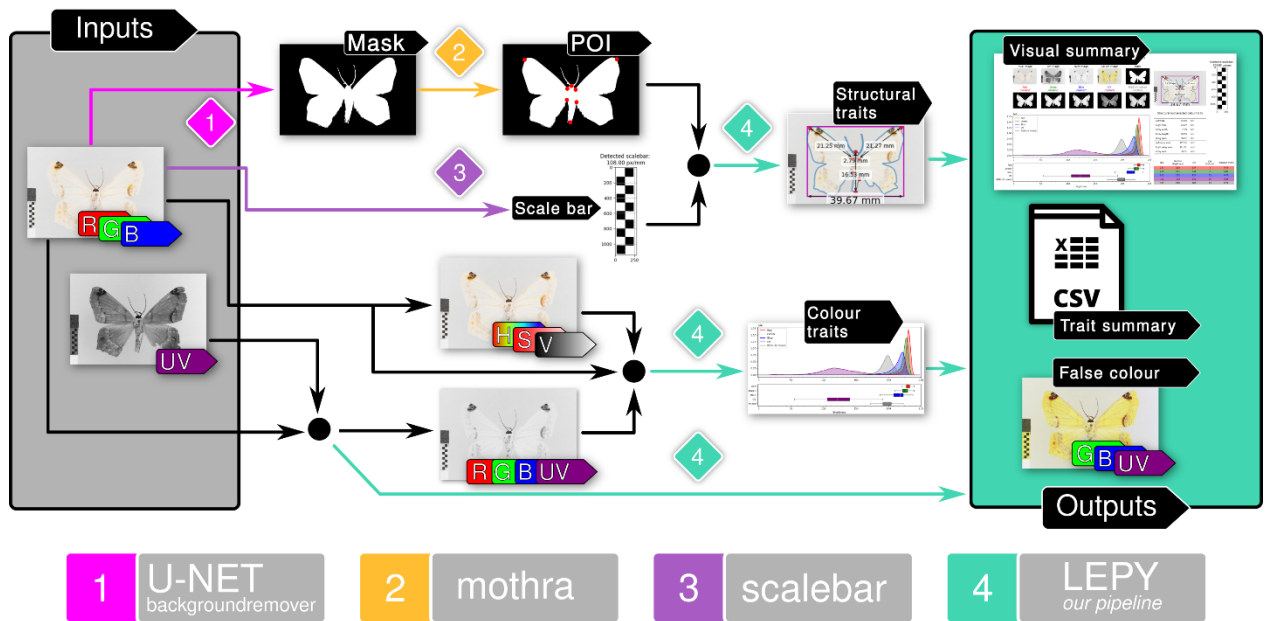
131 LEPY is an open-source pipeline hosted on GitHub (<https://github.com/tzlr-de/LEPY>),
132 developed and tested under Python 3.9 and 3.12. The recommended installation includes the
133 setup of a virtual python environment like Anaconda (Anaconda, 2023) and the installation of
134 the packages listed in the requirements file. For the detailed installation instructions, we refer
135 to the README.md in the code repository.

136 LEPY is a command-line program. To run the pipeline, the users must provide the image folder
137 and a configuration file with processing parameters as command-line arguments. In the code
138 repository, we included a configuration file with default values, which worked well on our
139 dataset.

140 A minimum of one regular (RGB) TIF image is required. For the inclusion of UV information,
141 the corresponding UV image must share the same file name as the RGB image, with 'uv'
142 appended to the UV file name (e.g., Pe-Geo-0016.tif and Pe-Geo-0016uv.tif; see Figure 3).
143 The images should preferably have good lighting conditions, including a neutral grey and
144 homogeneous background, consistent scaling across all images, and the removal of any labels
145 for photography (Brehm, 2025; Figure 3).

146 Using the UV channel, LEPY generates two new images: *RGB-UV mixed* and *GB-UV*. The
147 first image is a single-channel image, where each pixel is a weighted sum of the R, G, B, and
148 UV channels. It is related to the computation of a grayscale image; in such a normal grayscale
149 image, the grey value is $= 0.299 * \text{red} + 0.587 * \text{green} + 0.114 * \text{blue}$, corresponding to the
150 sensitivity of a human eye. Since we could not simply extend this weighting to the UV channel,
151 we decided for the most neutral approach in which all four channels were equally weighted
152 (0.25 each). The second image is a false colour image. In this image, the information from the
153 GB-UV channels is shown in the available RGB channels, resulting in the *GB-UV* image.

154



155

156 FIGURE 1 LEPY Pipeline - The input images are processed in multiple steps, including a CNN-based
 157 pixel-accurate segmentation of the specimen, the localisation of points of interest (POI) using the mothra
 158 package, the detection and processing of the scale bar using the scalebar package, and finally the
 159 computation of various structural and colouring traits. Besides the main trait summary, which LEPY
 160 stores as a CSV table, LEPY stores for each image a visual summary (see Section 3.1), a false colour
 161 image (GB-UV), all the computed traits in a JSON file, and the contours of the segmentation mask.

162 In Figure 1, we show the major processing steps of LEPY: (1) the pixel-accurate segmentation
 163 of the specimen, (2) the localisation of the points of interest (POI), (3) the detection and
 164 analysis of the scale bar, and (4) the computation of the structural and colouring traits based
 165 on the scale bar information and the POI.

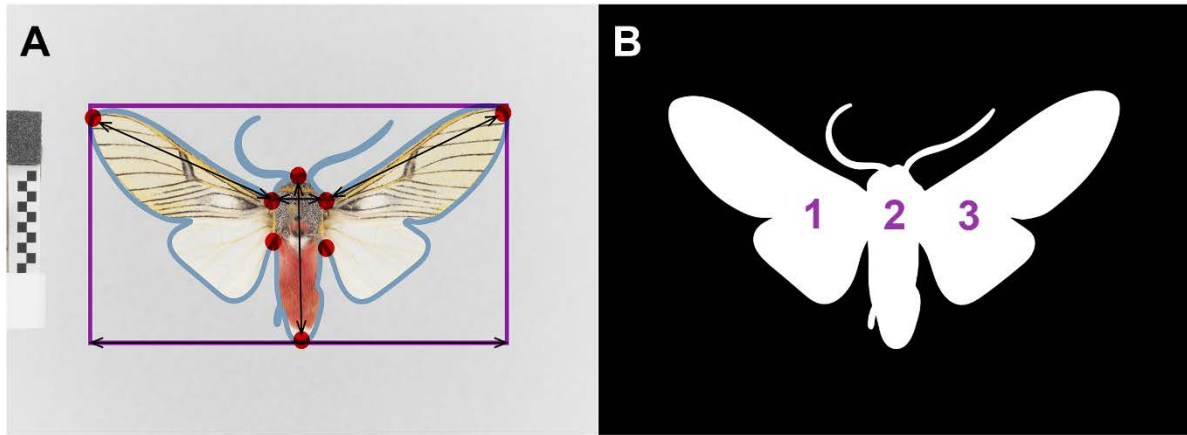
166 For the first step, we used the backgroundremover ([https://github.com/nadermx/](https://github.com/nadermx/backgroundremover)
 167 [backgroundremover](https://github.com/nadermx/backgroundremover)) package. It utilises a U-NET-based (Ronneberger et al., 2015) neural
 168 network which is trained for general background removal. This solution works well with the
 169 homogeneous light grey background we used (see Brehm, 2025), as the specimen can be
 170 usually easily distinguished from the background. We also evaluated other methods for
 171 background separation, e.g., GrabCut (Rother et al., 2004), Otsu's thresholding (Otsu, 1979),
 172 etc.), but the backgroundremover package delivered the most stable results, especially in the
 173 cases where the specimen had a very bright colouring. After postprocess the binary mask

174 returned by the backgroundremover by filling minor holes, we identify contours in the binary
175 mask and select only the largest contour under the assumption that this contour encloses the
176 specimen.

177 Based on the extracted binary mask, we estimated eight points of interest (POI) in each
178 specimen (Figure 2A), which helps to separate the body from the wings and calculate the sizes
179 of different specimen parts. We used and extended the Mothra package (Wilson et al., 2023),
180 which estimates four of the POI we are interested in, i.e., the wing tips and base of both
181 forewings. LEPY also estimates also the two lower points which connect the wings with the
182 body, and the upper and lower tips of the body (Figure 1).

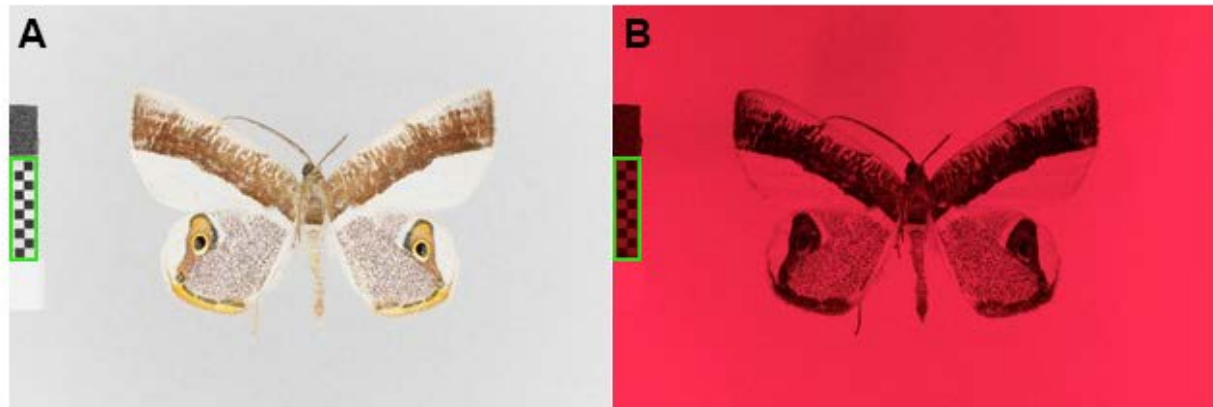
183 Next, for the extraction of the scaling information from the scale bar present in the image, we
184 used scalebar (<https://github.com/DiKorsch/scalebar>), a reworked and improved version of the
185 MothSeg pipeline (<https://github.com/erodner/mothseg>). To locate the scale bar, it uses a
186 simple pattern matching method
187 (https://docs.opencv.org/4.x/d4/dc6/tutorial_py_template_matching.html) by matching a
188 template image at different sizes (ranging from 2.5% to 100% of the original template size in
189 steps of 2.5%) across the left 15% area of the image. As a template, we used a single image
190 of a chessboard reference (see Figure 3) with a pre-computed ratio of 290 pixels per mm (a
191 scale bar template is supplied in S14; if printing, ensure it's at 100% for accurate
192 measurements; scale purchased from Sphere Optics, [https://sphereoptics.de/uebersicht-
193 produkte/](https://sphereoptics.de/uebersicht-produkte/)). Using this pre-computed scale and the resize factor matched best during pattern
194 matching, the final scale is computed and returned. If the scale of the template image is
195 unknown, then another algorithm identifies up to 50 corners of the chessboard and estimates
196 the scale based on the distances between these corners. Both the location of the template
197 image and the pre-computed scale can be modified in the configuration file if our provided
198 scale does not accurately represent the scale bar of the analysed images.

199



200
201 FIGURE 2 A: Points of interest (POI, shown as red dots) detected on a binarized moth image,
202 highlighting the body and length of both forewings, and the thorax width generated by the pipeline. B:
203 The binarized moth image is segmented into three sections: 1. the left forewing and hindwing, 2. the
204 body, and 3. the right forewing and hindwing.

205 Finally, after we estimated the eight POI and the scale of the image, LEPY quantifies various
206 structural and coloration traits. For structural measurements, it assesses thorax width, body
207 length, and forewing length (Figure 2A). By segmenting the mask into distinct body and wing
208 regions, LEPY also calculates their respective areas (Figure 2B). These measurements are
209 recorded in the visual summary generated for each image and the corresponding .csv file (see
210 2.2). For the colouring traits, LEPY analyses each channel of the RGB (red, green, and blue)
211 image separately. LEPY transforms the RGB image into HSV (hue, saturation, and value)
212 colour space. A distinguishing feature of LEPY is its capability to compute statistical metrics
213 for the ultraviolet (UV) channel. Finally, using the segmentation mask estimated in previous
214 image processing step, we calculate mean, median, minimum, and maximum pixel values for
215 the RGB-UV and HSV. For the all four channels (RGB-UV), LEPY calculates the 25% quartile,
216 75% quartile, the interquartile range (IQR) which represents dynamic range / contrast,
217 Shannon index, luminance, and chromaticity (formulas detailed in S11). In the visual summary,
218 we also add density and box plots for each channel and the *RGB-UV mixed* image (Figure 4).



219

220 FIGURE 3 Example of a pair of original images of a moth (Geometridae: *Opisthoxia* sp.), taken with a
 221 modified camera, UV lens and respective lighting and filtering (Brehm 2025). A: normal RGB
 222 photograph. B: UV photograph in which the red channel is the most sensitive to UV. A 10 mm scale bar
 223 with chessboard pattern is placed along the left edge for accurate and reliable size reference (green
 224 box).

225 2.2 | Pipeline outputs

226 The LEPY pipeline generates a new folder to store all result files. These files are saved in a
 227 directory specified by the command-line argument (--output). If this argument is omitted, the
 228 results are saved by default in a new created folder within the same directory of the input folder.
 229 This folder is named after the input folder, with "_results" appended to the name.

230 The primary result file is a trait summary document in CSV format, containing all traits
 231 calculated by LEPY. Each row represents a single input image, with structural and coloration
 232 traits stored in separate columns (for detailed descriptions, see SI1).

233 Besides the trait summary file, the current version of LEPY creates the following outputs: (1) a
 234 contour of the segmentation mask, (2) a false colour image (if the UV-channel was detected;
 235 GB-UV), (3) a trait file in JSON format containing the same structuring and colouring traits as
 236 the corresponding row in the CSV summary file, and (4) a visual summary of the main structural
 237 and colouring traits, and of the different colour channels in form of density and box plots. The
 238 visual summary is explained in more detail in Section 3.1. Each of these outputs is stored in a
 239 separate subfolder: "contours", "gbuv", "json", and "visualisations", respectively.

240

241 **2.3 | Validation of structural trait measurements and performance in an** 242 **example dataset**

243 We performed a validation of size measurements derived from LEPY against a traditional
244 manual method, using ImageJ, a widely used software for morphometric analysis (Rasband,
245 2015). For this, we used a dataset of 100 moth images of moths of the families Sphingidae (54
246 images) and Saturniidae (46 images; See SI2). Moths were sampled in Peru in 2022 and 2023
247 as part of the ANDIV project (Holzmann et al., 2025). Moths were collected at 26 sampling
248 sites between 250 and 3650 m a.s.l. in habitats ranging from Amazon lowland rainforest up to
249 the treeline in the Andes. Size measurements included forewing length (both sides), body width
250 (BW), body length (BL), and wingspan (WS). We applied paired Welch's t test when normality
251 assumptions were met, and a Wilcoxon rank sum test when deviations were detected. We
252 checked the normality of model residuals using the Shapiro-Wilk test. Statistical significance
253 was determined at a threshold of $p < 0.05$.

254 Furthermore, we explored selected morphological traits (size and colour) using data derived
255 from LEPY. This also included moths from the same taxa collected in the same region as
256 above. A total of 224 photographed moth specimens with 109 image pairs of Saturniidae and
257 115 image pairs of Sphingidae were analysed (See SI3). Photographs were taken at the
258 Phyletisches Museum Jena (PMJ), Germany, according to the methods of photography and
259 lighting described in detail by Brehm (2025). LEPY was run on a computer with an Intel(R)
260 Core (TM) i5-13500 2.50GHz processor and 16.0 GB RAM (15.7 GB usable). As an example
261 of the software's ecological application, we investigated the relationship between elevation and
262 several functional traits, including forewing length, wing area and colour properties such as
263 brightness (median of the four colour channels) and dynamic range / contrast (expressed as
264 interquartile range of four colour channels).

265 Statistical analyses for the validation and exploration of performance were conducted in R
266 v.4.4.0 (R Core Team, 2024). To evaluate whether elevation had a linear or non-linear effect

267 on the traits, we constructed generalized additive models (GAMs) separately for each
268 taxonomic family and trait. In GAMs, non-parametric smoothers are used to define the
269 relationship between a response and a predictor variable, allowing flexible, semi-automatic
270 estimations of both linear and non-linear relationships. To avoid overparameterization, we set
271 the basis dimension of the smoothing term (k) to five for all GAMs. The models were
272 implemented using the 'mgcv' package (Wood, 2023).

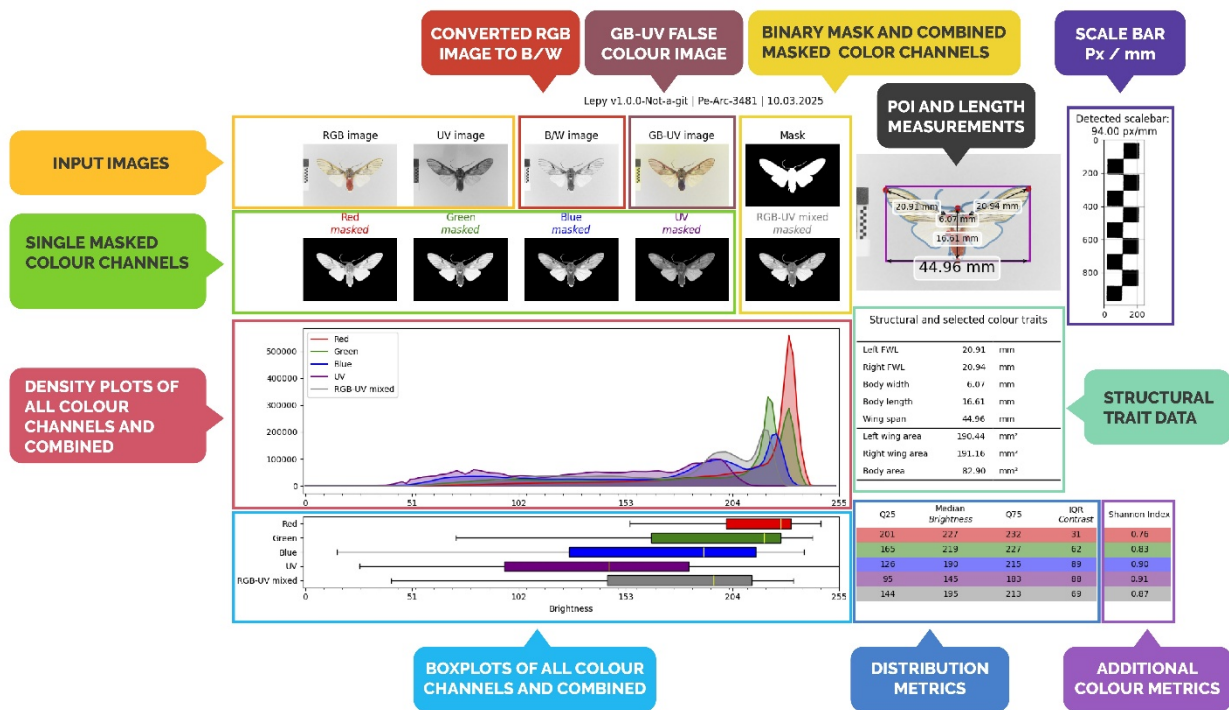
273

274 The number of images LEPY can process in one run depends on the computer's memory
275 capacity. To address this, we developed a script called LepyLoop, for analysing large datasets
276 (available at <https://github.com/DesBoe/LepyLoop>). This script must be run in the same
277 environment as LEPY. It will ask users for an input directory containing images or subfolders.
278 All images are stored in a new folder and checked for unmatched RGB and UV image pairs.
279 Small packages are created that contain a smaller number of images to be analysed
280 consecutively by LEPY. Users can specify the individual count for each package (we
281 recommend 100 from computational capacity). After all packages are analysed, input images
282 are stored in their original directory, results are merged, and a .xlsx file containing all statistics
283 is generated.

284 **3 | RESULTS**

285 **3.1 | Visual summary**

286 As described in Section 2.2, LEPY creates a variety of output files after processing the images.
287 The most condensed summary is the visual summary as explained in Figure 4. It visualises
288 the most important structural and colouring traits, different colour channels (including the UV
289 channel), as well as statistics of each channel in the form of density and box plots. The visual
290 summary is both useful and practical, as it displays the main traits generated by LEPY and
291 provides a quick check to ensure that the measurements and all LEPY steps were executed
292 correctly for each image.



294

295 FIGURE 4 Example of a visual summary of the results of LEPY for a moth specimen (Arctiinae: *Idalus*
 296 sp.) with explanations (coloured boxes). The visualisation shows the input images (orange), the binary
 297 mask (yellow), the POI, and the scale bar (purple). It also shows structural trait data (blue green), density
 298 plots (pink), and boxplots (light blue) of four colour channels with colour metrics for each (blue), and the
 299 Shannon index (violet). The density plots indicates that the moth has relatively high brightness values
 300 in all channels (in the order red, green, blue, and ultraviolet). The boxplots visualise the interquartile
 301 range (IQR) of the dynamic range / contrast. The bars of the green, blue and UV channel are relatively
 302 broad, i.e., they have a wide dynamic range / contrast. The red bar is rather narrow, indicating lesser
 303 dynamic range / contrast in the red channel (See SI1 for further explanation of colour metrics).

304

305 In the upper left part, it displays a series of images. From left to right in the first row those are
 306 the original input images, the UV (ultraviolet) channel, classic grayscale image (B/W; black and
 307 white), the false colour image (*GB-UV*) as described in Section 2.1, and finally the binary mask
 308 estimated with the backgroundremover package. In the second row the images from left to
 309 right are four channels masked according to the binary mask and the weighted average of

310 those channels, the *RGB-UV mixed* image. In the upper right section, the estimated points of
311 interest (POI), the length measurements of the specimen, and the detected scale bar along
312 with the estimated pixel scale in pixel per millimetre are visualised.

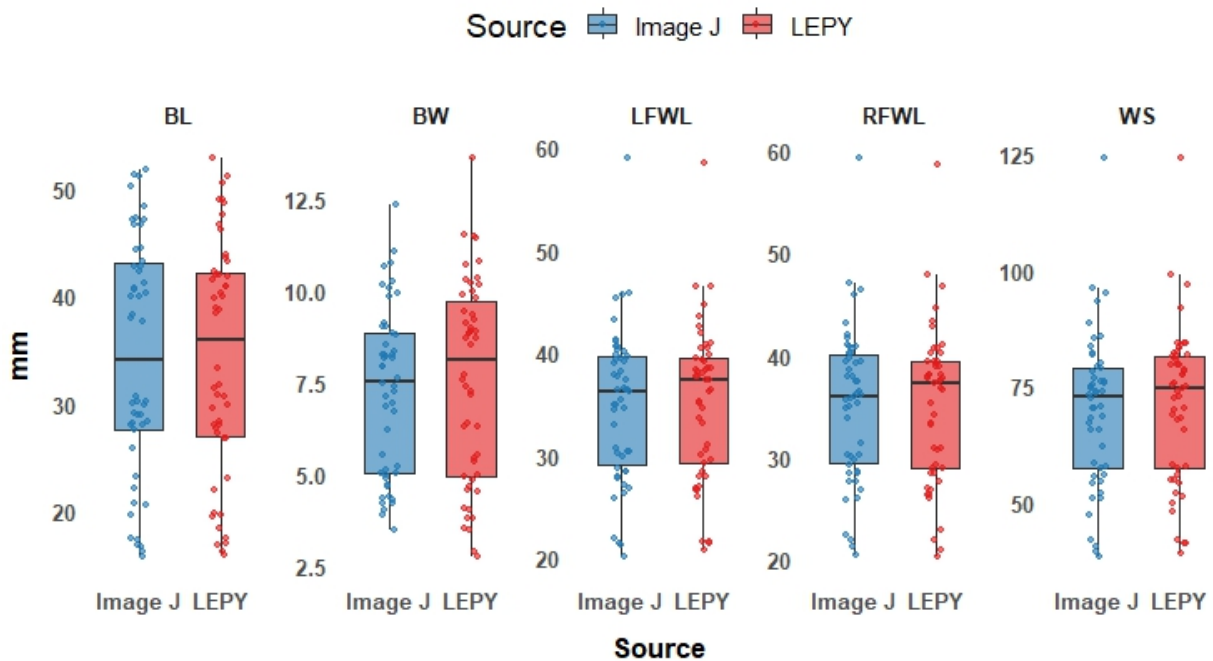
313 The lower part of the visual summary displays the density and box plots of the four colour
314 channels and the *RGB-UV mixed* image on the left. The most important structural and colour
315 traits of the specimen are displayed in two tables on the right. Based on the eight POI, LEPY
316 calculates eight structural traits: five lengths and three areas as shown in the visual summary
317 (Figure 4). The colour traits include the median, Q25, Q75, IQR (interquartile range), and the
318 Shannon index of the four channels and of the *RGB-UV mixed* image. The median pixel value
319 is a measure for the brightness of each channel. The dynamic range / contrast of an image is
320 usually defined by the difference between maximum and minimum pixel value. We use the
321 IQR of the dynamic range / contrast because it is less sensitive to statistical outliers and
322 therefore probably provides more stable results. As mentioned in Section 2.2, additional
323 colouring traits are stored in the main trait summary file. Those are explained in more detail in
324 supplementary information (SI).

325

326 **3.2 | Validation of structural trait measurements**

327 The comparison between LEPY and ImageJ measurements ($n = 100$) revealed no statistically
328 significant differences for any of the measured parameters. For normally distributed data (both
329 forewing lengths), Welch's t-tests produced p -values of 0.80 and 0.96, respectively. For non-
330 normally distributed data (BW, BL, and WS), Wilcoxon rank-sum tests resulted in p -values of
331 0.50, 0.85, and 0.49, respectively. Visual representation of the data, presented in boxplots,
332 further supported the similarity between the two measurement methods (Figure 5).

333



334

335 FIGURE 5 Comparison of structural measurements obtained using ImageJ and LEPY. Boxplots with
 336 jittered points represent measurements for body length (BL), body width (BW), left forewing length
 337 (LFWL), right forewing length (RFWL), and wingspan (WS) across the two methods.

338 3.3 | Performance of LEPY in the example data set

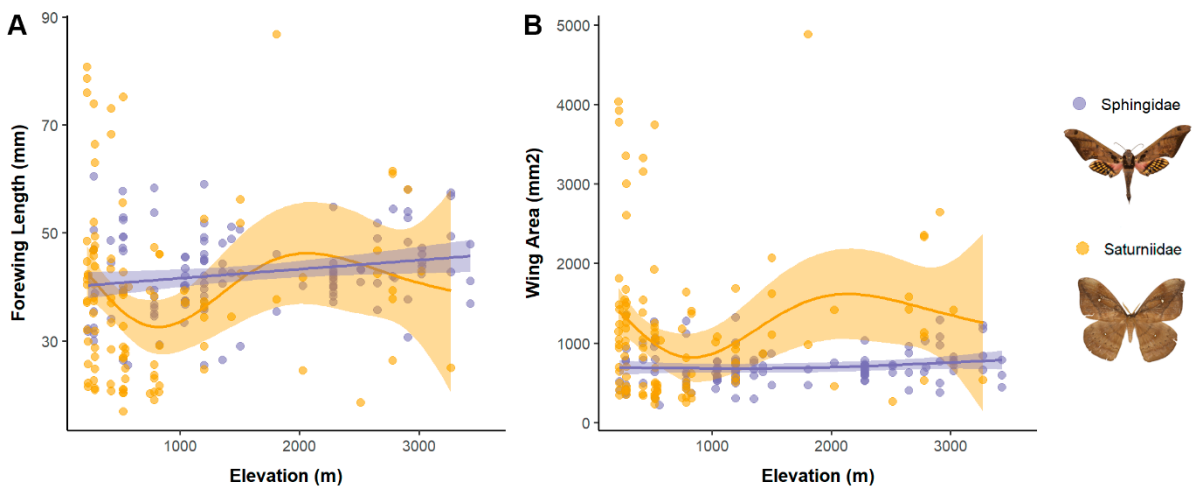
339 *General performance.* The processing of 224 image pairs (RGB image, UV image) took
 340 between 15 and 50 seconds per pair. The performance of LEPY is influenced by specific image
 341 and specimen characteristics. For example, visible antennae or legs in the images occasionally
 342 led to errors in POI identification, resulting in inaccuracies in morphological measurements.
 343 Specimen preparation and mounting also played a role: errors in wing positioning, such as
 344 misalignment of the wings at a 90° angle relative to the body or asymmetry between the two
 345 sides of the body, led to POI detection errors.

346

347 *Forewing length and wing area.* The effect of elevation on forewing length and wing area varied
 348 between Sphingidae and Saturniidae, as indicated by the Generalised Additive Models (GAM).
 349 For forewing length, elevation had a significant effect in both families, but the trend of this
 350 relationship differed. In Sphingidae, the effect was linear (edf = 1, F = 5.227, p = 0.0241),

351 though the model explained only 4.42% of the deviance. In Saturniidae, the effect was non-
 352 linear (edf = 3.281, $F = 2.267$, $p = 0.0487$), and the model explained a slightly higher proportion
 353 of variance (10% deviance explained). These results suggest that elevation influences
 354 forewing length in both families, but with a non-linear effect in Saturniidae (Figure 6A). For
 355 wing area, elevation had no significant effect in either family. In Sphingidae, the relationship
 356 was non-significant (edf = 1.58, $F = 1.562$, $p = 0.267$ deviance explained = 2.91%). In
 357 Saturniidae, wing area changed in a complex manner with elevation, but the effect was only
 358 marginally significant (edf = 3.183, $F = 2.205$, $p = 0.0579$, explained deviance = 9.4%). These
 359 results suggest that elevation has a limited effect on wing area variation in both families, though
 360 Saturniidae shows a slightly stronger non-linear response (Figure 6B).

361

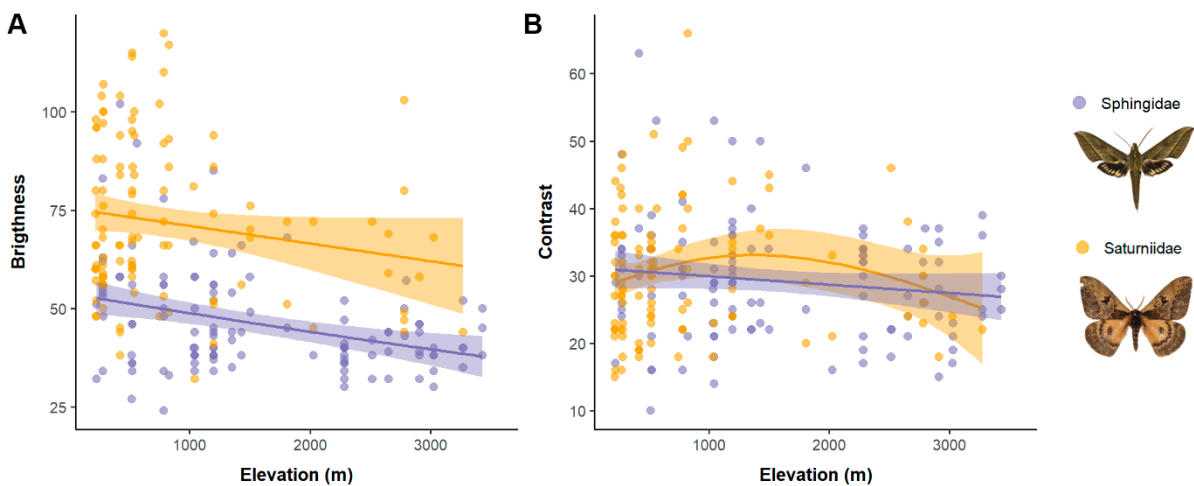


362

363 FIGURE 6 A. Relationship between elevation and forewing length of Sphingidae (purple) and
 364 Saturniidae (orange). B. Relationship between elevation and wing area of Sphingidae (purple) and
 365 Saturniidae (orange). Each point represents an individual moth, and the shaded regions indicate 95%
 366 confidence intervals around the fitted GAM predictions (lines).

367 *Brightness and dynamic range / contrast.* The effect of elevation on brightness and dynamic
 368 range / contrast was weak in both Sphingidae and Saturniidae. For brightness, elevation had
 369 a significant effect in Sphingidae (edf = 1.083, $F = 12.05$, $p = 0.000384$), suggesting a nearly
 370 linear relationship. The model explained 11.5% of the deviance, indicating that elevation
 371 played a moderate role in shaping this trait in Sphingidae. In Saturniidae, trends in brightness

372 were similar but the effect was not significant (edf = 3.216, $F = 1.62$, $p = 0.129$). The model
 373 explained only 7.53% of the deviance, suggesting a minimal impact of elevation on brightness
 374 in this family (Figure 7A). For dynamic range / contrast, elevation had a non-significant effect
 375 in both families. In Sphingidae, the model showed a weak relationship with elevation (edf = 1,
 376 $F = 2.106$, $p = 0.149$), explaining only 1.83% of the deviance. Similarly, for Saturniidae, the
 377 effect was weak and non-significant (edf = 1.917, $F = 1.675$, $p = 0.194$), with 4.56% of the
 378 deviance explained. These results suggest that elevation had little influence on contrast
 379 variation in both families (Figure 7B).
 380



381
 382 FIGURE 7 A. Relationship between elevation and brightness (median of four colour channels) in
 383 Sphingidae (purple) and Saturniidae (orange). B. Relationship between elevation and dynamic range /
 384 contrast (IQR of four colour channels) in Sphingidae (purple) and Saturniidae (orange). Points represent
 385 individual data, and the shaded regions indicate confidence intervals around the fitted GAM predictions
 386 (lines).

387 4 | DISCUSSION

388 4.1 | Capabilities of LEPY

389 LEPY demonstrated significantly enhanced capabilities compared to previous algorithms such
 390 as Mothseg and Mothra. LEPY can easily analyse more than thousand image pairs overnight

391 with a normal computer and provides a wealth of data for analysing traits of body size and
392 colouration of moths and butterflies at once. Results automatically derived by LEPY were
393 highly like those measured manually with ImageJ. Our examples showed only a selection of
394 the possibilities and demonstrate that different size measurements can lead to different results.
395 For example, a longer wing length does not automatically mean a larger wing area, as this
396 ratio varies between different taxa. In many studies, only a single measure, such as wing
397 length, was used, but this is only possible if the groups are relatively homogeneous (e.g.,
398 Brehm et al., 2019).

399 With the automated methods used in LEPY, it is now easy to record different measures
400 simultaneously and compare them. The comparison of colouration parameters such as
401 brightness only give a foretaste of future possibilities. In our tested dataset, members of both
402 families become darker with elevation whereas we found no significant changes in the dynamic
403 range /contrast. These results highlight how morphological traits can vary in response to
404 environmental gradients. Stronger patterns are expected in groups with aposematic or
405 chemically defended species, such as butterflies and Arctiinae and other moths, which use
406 coloration to signal toxicity or unpalatability (Prudic et al., 2007).

407 The inclusion of UV information represents a significant further development. UV patterns can
408 be important for communication, camouflage, and mating signals (Pinna et al., 2021;
409 Prabhulinga et al., 2022), but the systematic consideration of UV information has received little
410 attention to date, e.g., in digitisation programmes (Brehm, 2025). To better understand this
411 potential, we encourage studies to compare the contribution that this information can make.
412 LEPY can also be used without UV photographs and represents the traditional parameters
413 such as HSV (hue, saturation, and intensity). Our four-channel approach enables the full
414 integration and visualization of UV information using false-colour images. We also encourage
415 to work on further models for this colour information and possibly derive further meaningful
416 parameters. LEPY provides scalable analyses of large Lepidoptera datasets, allowing the
417 accurate extraction of morphological traits relevant to studies of phenotypic diversity,
418 ecological adaptations, and trait-environment relationships. The comparison between LEPY

419 and ImageJ measurements demonstrated strong consistency across all measured
420 parameters, with no statistically significant differences observed. This suggests that LEPY
421 provides an accurate and automated alternative to ImageJ for morphological measurements
422 in Lepidoptera. Future studies could leverage LEPY to streamline data collection processes
423 while maintaining measurement accuracy. Data generated by LEPY can easily be registered
424 in publicly accessible repositories.

425

426 **4.2 | Current limitations of LEPY**

427 Despite its strengths, LEPY has some limitations that may require further development for
428 other types of input data, for example regarding the type of scale bar used. LEPY currently
429 requires a specific chessboard pattern. Adapting to different scales or formats would require
430 additional programming, which in most cases appears possible, given a standardization (e.g.,
431 a uniform 10 mm black scale bar). Furthermore, extending compatibility to a broader range of
432 file formats could enhance a broader accessibility and usability. Accuracy and efficiency of the
433 pipeline are dependent on the quality of specimen preparation. Errors in segmentation and
434 POI detection can arise from poorly prepared specimens, visible legs, or pale or translucent
435 wings. Such problems can never be completely avoided but the visual summary of results
436 make it possible to identify such errors relatively quickly and replace them with manual
437 measurements.

438 A broader question is whether LEPY could be adapted in such a way that it will be possible to
439 investigate also other insect groups. Although this is certainly desirable, we expect that insects
440 characterized by pronounced three-dimensional body shapes will be more difficult to analyse,
441 and additional technologies (such as image stacking) are likely to be required. However, LEPY
442 could serve as a good starting point, as its modularity and extensibility are likely to allow such
443 adaptations.

444 **4.3 | Ecological relevance and potential applications of LEPY**

445 LEPY enables the study of Lepidoptera adaptation to environmental changes, such as climate
446 change or habitat loss (Clusella-Trullas & Nielsen, 2020; Duarte et al., 2017; Henriques et al.,
447 2022). For example, body size is related to individual mobility, whereas individuals with
448 reduced mobility tend to be more sensitive to habitat loss (Mattila et al., 2008). The tool enables
449 the monitoring of changes in Lepidoptera populations and communities over time. By
450 facilitating the study of how environmental changes and habitat degradation influence their
451 morphology, coloration, and survival, it provides critical insights into species responses. Such
452 information is essential for predicting whether species will adapt or face decline, as well as for
453 informing the development of effective conservation strategies (Koneru & Caro, 2022; Mikitová
454 et al., 2022).

455 In our example dataset, morphological traits varied with elevation, likely due to associated
456 environmental changes. However, the magnitude and direction of these effects differed by trait.
457 Notably, forewing length increased significantly with elevation, particularly in Sphingidae. In
458 contrast, Saturniidae species had significantly larger wing areas, but this trait did not follow a
459 clear elevational pattern. These findings align with those of Brehm et al. (2019), who found a
460 significant increase in body size (measured as forewing length) along an elevational gradient
461 of nearly 2,900 meters in Costa Rica, with temperature as the main predictive factor. However,
462 Brehm & Fiedler (2004) reported a negative relationship between body size and elevation of
463 Geometridae moths in Ecuador along a gradient of more than 1,600 m, suggesting that
464 geographical differences and gradient length may influence these patterns.

465 The increase in forewing length at higher elevations may reflect adaptations to flight constraints
466 in montane environments. Reduced atmospheric pressure may require larger wings to
467 maintain efficient flight (Brehm et al., 2019). The relatively low R^2 for forewing length suggests
468 that while elevation has an effect, other factors – such as taxon-specific adaptations or
469 phylogenetic relationships – are likely to contribute to variation in this trait. In contrast, traits
470 with higher R^2 values (brightness and wing area), indicate that moth taxon and, to some extent,

471 elevation explain most of the variation. These results support previous findings that colour-
472 related traits change with elevation (Fiedler & Brehm, 2021).

473 Previous studies found that larger and darker insects are favoured in colder environments and
474 that body size and coloration might play an important role for thermoregulation, even in
475 nocturnal species. For instance, Heidrich et al. (2018) found that noctuid moths were larger
476 and darker at high elevations in Europe, whereas geometrids showed an opposite trend in
477 brightness and no clear trend in body size.

478 For future research, integrating morphological patterns with phylogenetic analyses would help
479 to clarify whether the observed changes are primarily driven by elevation or result from
480 species-specific evolutionary adaptations. Combining trait-based approaches with
481 phylogenetic frameworks will be essential for understanding how moth communities respond
482 to environmental gradients over evolutionary timescales (Shrestha et al., 2014).

483 **5 | CONCLUSION**

484 LEPY is a tool that addresses key challenges in Lepidoptera trait research by automating the
485 analysis of structural traits and colour properties, including UV information, across large
486 datasets of specimens and/or images. Our results highlight the effectiveness of LEPY in
487 quantifying morphological trait variation and detecting the influence of elevational gradients on
488 Lepidoptera communities. By incorporating both morphological and ecological data, this
489 approach can provide valuable insights into how environmental factors shape trait distributions
490 in insect communities. We encourage users to test LEPY and expand its possibilities through
491 further adaptation steps.

492 **AUTHOR CONTRIBUTIONS**

493 Yenny Correa-Carmona, Dennis Böttger, Dimitri Korsch, and Gunnar Brehm conceptualised
494 and developed the LEPY pipeline, contributing to both its design and the manuscript's content
495 and revisions. Dimitri Korsch implemented the pipeline code. Yenny Correa-Carmona drafted

496 the initial manuscript and conducted the validation data analysis with advice from Marcell
497 Peters. Gunnar Brehm organized the example dataset and took all photographs. All authors
498 reviewed and approved the final version of the manuscript.

499 **ACKNOWLEDGEMENTS**

500 We would like to thank all people involved in the ANDIV project field work in Peru, especially
501 ACCA (Amazon Conservation Association) and the staff of the stations, the ABERG project
502 (the Andes Biodiversity and Ecosystem Research Group), our field assistants, the MUBI and
503 ICNDMB biological collections who gave us their support, the SERNANP for the access to the
504 Manu National Park (N° 18-2022-SERNANP-JEF) and the SERFOR for the research permits
505 (N° D0010444). We also thank all the staff of the Phyletisches Museum in Jena (Germany),
506 and all students involved in the ANDIV project. Research was funded by the Deutsche
507 Forschungsgemeinschaft (BR 2280/9-1 (PAK 1034/1)).

508 **CONFLICT OF INTEREST STATEMENT**

509 The authors have no conflict of interest.

510 **DATA AVAILABILITY STATEMENT**

511 Code used for this study are available from the GitHub repository at <https://github.com/tzlr->
512 [de/LEPY](https://github.com/tzlr-de/LEPY).

513 **ORCID**

514 Yenny Correa-Carmona <https://orcid.org/0000-0003-0209-8729>

515 Dennis Böttger <https://orcid.org/0000-0002-9593-7968>

516 Dimitri Korsch <https://orcid.org/0000-0001-7187-1151>

517 Kim L. Holzmann <https://orcid.org/0000-0002-2469-6212>

518 Pedro Alonso-Alonso <https://orcid.org/0000-0001-8791-5227>

519 Andrea Pinos <https://orcid.org/0009-0007-0275-8172>

520 Felipe Yon <https://orcid.org/0000-0002-5667-873X>
521 Alexander Keller <https://orcid.org/0000-0001-5716-3634>
522 Ingolf Steffan-Dewenter <https://orcid.org/0000-0003-1359-3944>
523 Marcell K. Peters <https://orcid.org/0000-0002-1262-0827>
524 Gunnar Brehm <https://orcid.org/0000-0002-7599-2847>

525 REFERENCES

526 Anaconda, Inc. (2023). *Anaconda Navigator*. The Desktop Portal to Data Science.
527 Bálint, Z., Kertész, K., Piszter, G., Vértessy, Z., & Biró, L. P. (2012). The well-tuned
528 blues: The role of structural colours as optical signals in the species recognition
529 of a local butterfly fauna (Lepidoptera: Lycaenidae: Polyommatainae). *Journal of*
530 *the Royal Society Interface*, 9(73), 1745–1756.
531 <https://doi.org/10.1098/rsif.2011.0854>
532 Brehm G (accepted). Light in standardised insect photography and description of
533 lighting devices, including the UV range. *Nota lepidopterologica*.
534 Brehm, G., & Fiedler, K. (2004). Bergmann's rule does not apply to geometrid moths
535 along an elevational gradient in an Andean montane rain forest. *Global Ecology*
536 *and Biogeography*, 13(1), 7–14. [https://doi.org/10.1111/j.1466-](https://doi.org/10.1111/j.1466-882X.2004.00069.x)
537 [882X.2004.00069.x](https://doi.org/10.1111/j.1466-882X.2004.00069.x)
538 Brehm, G., Niermann, J., Jaimes Nino, L. M., Enseling, D., Jüstel, T., Axmacher, J.
539 C., Warrant, E., & Fiedler, K. (2021). Moths are strongly attracted to ultraviolet
540 and blue radiation. *Insect Conservation and Diversity*, 14(2), 188–198.
541 <https://doi.org/10.1111/icad.12476>
542 Brehm, G., Zeuss, D., & Colwell, R. K. (2019). Moth body size increases with
543 elevation along a complete tropical elevational gradient for two hyperdiverse
544 clades. *Ecography*, 42(4), 632–642. <https://doi.org/10.1111/ecog.03917>

545 Chown, S. L., & Gaston, K. J. (2010). Body size variation in insects: A
546 macroecological perspective. *Biological Reviews*, 85(1), 139–169.
547 <https://doi.org/10.1111/j.1469-185X.2009.00097.x>

548 Clusella-Trullas, S., & Nielsen, M. (2020). The evolution of insect body coloration
549 under changing climates. *Current Opinion in Insect Science*, 41, 25–32.
550 <https://doi.org/10.1016/j.cois.2020.05.007>

551 Correa-Carmona, Y., Rougerie, R., Arnal, P., Ballesteros-Mejia, L., Beck, J.,
552 Dolédec, S., Ho, C., Kitching, I. J., Lavelle, P., Le Clec'h, S., Lopez-Vaamonde,
553 C., Martins, M. B., Murienne, J., Oszwald, J., Ratnasingham, S., & Decaëns, T.
554 (2022). Functional and taxonomic responses of tropical moth communities to
555 deforestation. *Insect Conservation and Diversity*, 15(2), 236–247.
556 <https://doi.org/10.1111/icad.12549>

557 Cortés-Gómez, A. M., González-Chaves, A., Urbina-Cardona, N., & Garibaldi, L. A.
558 (2023). Functional Traits in Bees: the Role of Body Size and Hairs in the
559 Pollination of a Passiflora Crop. *Neotropical Entomology*, 52(4), 642–651.
560 <https://doi.org/10.1007/s13744-023-01058-w>

561 Cronin, T. W., & Bok, M. J. (2016). Photoreception and vision in the ultraviolet. In
562 *Journal of Experimental Biology*, 219 (18), 2790–2801.
563 <https://doi.org/10.1242/jeb.128769>

564 Duarte, R. C., Flores, A. A. V., & Stevens, M. (2017). Camouflage through colour
565 change: Mechanisms, adaptive value and ecological significance. *Philosophical
566 Transactions of the Royal Society B: Biological Sciences*, 372(1724), 20160342.
567 <https://doi.org/10.1098/rstb.2016.0342>

568 Feng, L., Bhanu, B., & Heraty, J. (2015). Identification and Retrieval of Moth Images
569 Based on Wing Patterns. *Video Bioinformatics: From Live Imaging to
570 Knowledge*, 349–369. https://doi.org/10.1007/978-3-319-23724-4_19

571 Fiedler, K., & Brehm, G. (2021). Aposematic coloration of moths decreases strongly
572 along an elevational gradient in the Andes. *Insects*, 12(10), 903.
573 <https://doi.org/10.3390/insects12100903>

574 Fountain-Jones, N. M., Baker, S. C., & Jordan, G. J. (2015). Moving beyond the guild
575 concept: Developing a practical functional trait framework for terrestrial beetles.
576 *Ecological Entomology*, 40(1), 1–13. <https://doi.org/10.1111/een.12158>

577 Freitas, A. V. L., Santos, J. P., Rosa, A. H. B., Iserhard, C. A., Richter, A., Siewert,
578 R. R., Gueratto, P. E., Carreira, J. Y. O., & Lourenço, G. M. (2020). Sampling
579 methods for butterflies (Lepidoptera). *Measuring Arthropod Biodiversity: A*
580 *Handbook of Sampling Methods*, 101–123. [https://doi.org/10.1007/978-3-030-](https://doi.org/10.1007/978-3-030-53226-0_5)
581 [53226-0_5](https://doi.org/10.1007/978-3-030-53226-0_5)

582 Gámez-Virúés, S., Perović, D. J., Gossner, M. M., Börschig, C., Blüthgen, N., De
583 Jong, H., Simons, N. K., Klein, A. M., Krauss, J., Maier, G., Scherber, C.,
584 Steckel, J., Rothenwöhrer, C., Steffan-Dewenter, I., Weiner, C. N., Weisser, W.,
585 Werner, M., Tschardtke, T., & Westphal, C. (2015). Landscape simplification
586 filters species traits and drives biotic homogenization. *Nature Communications*,
587 6(1), 8568. <https://doi.org/10.1038/ncomms9568>

588 Heidrich, L., Friess, N., Fiedler, K., Brändle, M., Hausmann, A., Brandl, R., & Zeuss,
589 D. (2018). The dark side of Lepidoptera: Colour lightness of geometrid moths
590 decreases with increasing latitude. *Global Ecology and Biogeography*, 27(4),
591 407–416. <https://doi.org/10.1111/geb.12703>

592 Henriques, N. R., Lourenço, G. M., Diniz, É. S., & Cornelissen, T. (2022). Is elevation
593 a strong environmental filter? Combining taxonomy, functional traits and
594 phylogeny of butterflies in a tropical mountain. *Ecological Entomology*, 47(4),
595 613–625. <https://doi.org/10.1111/een.13145>

596 Hill, G. M., Kawahara, A. Y., Daniels, J. C., Bateman, C. C., & Scheffers, B. R.
597 (2021). Climate change effects on animal ecology: butterflies and moths as a

598 case study. *Biological Reviews*, 96(5), 2113–2126.
599 <https://doi.org/10.1111/brv.12746>

600 Holzmann, K. L., Alonso-Alonso, P., Correa-Carmona, Y., Pinos, A., Yon, F., Brehm,
601 G., Keller, A., Steffan-Dewenter, I., & Peters, M. K. (2025). Cold waves in the
602 Amazon rainforest and their ecological impact. *Biology Letters*, 21(1),
603 20240591. <https://doi.org/10.1098/rsbl.2024.0591>

604 Høye, T. T., Ärje, J., Bjerge, K., Hansen, O. L. P., Iosifidis, A., Leese, F., Mann, H.
605 M. R., Meissner, K., Melvad, C., & Raitoharju, J. (2021). Deep learning and
606 computer vision will transform entomology. *Proceedings of the National
607 Academy of Sciences of the United States of America*, 118(2), e2002545117.
608 <https://doi.org/10.1073/PNAS.2002545117>

609 Jaimes Nino, L. M., Mörtter, R., & Brehm, G. (2019). Diversity and trait patterns of
610 moths at the edge of an Amazonian rainforest. *Journal of Insect Conservation*,
611 23(4), 751–763. <https://doi.org/10.1007/s10841-019-00168-4>

612 Koičková, L., Miklisová, D., Čanády, A., & Panigaj, L. (2012). Is colour an important
613 factor influencing the behaviour of butterflies (Lepidoptera: Hesperioidea,
614 Papilionoidea)? *European Journal of Entomology*, 109(3), 403.
615 <https://doi.org/10.14411/eje.2012.052>

616 Koneru, M., & Caro, T. (2022). Animal Coloration in the Anthropocene. *Frontiers in
617 Ecology and Evolution*, 10, 857317. <https://doi.org/10.3389/fevo.2022.857317>

618 Lamarre, G. P. A., Pardikes, N. A., Segar, S., Hackforth, C. N., Laguerre, M.,
619 Vincent, B., Lopez, Y., Perez, F., Bobadilla, R., Ramírez Silva, J. A., & Basset,
620 Y. (2022). More winners than losers over 12 years of monitoring tiger moths
621 (Erebidae: Arctiinae) on Barro Colorado Island, Panama. *Biology Letters*, 18(4),
622 20210519 . <https://doi.org/10.1098/rsbl.2021.0519>

623 Lyytinen, A., Lindström, L., & Mappes, J. (2004). Ultraviolet reflection and predation
624 risk in diurnal and nocturnal Lepidoptera. *Behavioral Ecology*, 15(6), 982–987.
625 <https://doi.org/10.1093/beheco/arh102>

626 Manoukis, N. C., & Collier, T. C. (2019). Computer vision to enhance behavioral
627 research on insects. *Annals of the Entomological Society of America*, 112(3),
628 227–235. <https://doi.org/10.1093/aesa/say062>

629 Mattila, N., Kotiaho, J. S., Kaitala, V., & Komonen, A. (2008). The use of ecological
630 traits in extinction risk assessments: A case study on geometrid moths.
631 *Biological Conservation*, 141(9), 2322–2328.
632 <https://doi.org/10.1016/j.biocon.2008.06.024>

633 Mikitová, B., Šemeláková, M., & Panigaj, L. (2022). Wing morphology and eyespot
634 pattern of *Erebia medusa* (Lepidoptera, Nymphalidae) vary along an elevation
635 gradient in the Carpathian Mountains. *Nota Lepidopterologica*, 45, 233–250.
636 <https://doi.org/10.3897/nl.45.68624>

637 Moraes, S. de S., Murillo-Ramos, L., Machado, P. A., Ghanavi, H. R., Magaldi, L. M.,
638 Silva-Brandão, K. L., Kato, M. J., Freitas, A. V. L., & Wahlberg, N. (2021). A
639 double-edged sword: Unrecognized cryptic diversity and taxonomic impediment
640 in *Eois* (Lepidoptera, Geometridae). *Zoologica Scripta*, 50(5), 633–646.
641 <https://doi.org/10.1111/zsc.12488>

642 Murillo-Ramos, L., Chazot, N., Sihvonen, P., Õunap, E., Jiang, N., Han, H., Clarke, J.
643 T., Davis, R. B., Tammaru, T., & Wahlberg, N. (2021). Molecular phylogeny,
644 classification, biogeography and diversification patterns of a diverse group of
645 moths (Geometridae: Boarmiini). *Molecular Phylogenetics and Evolution*, 162,
646 107198. <https://doi.org/10.1016/j.ympev.2021.107198>

647 Ohashi, K., Makino, T. T., & Arikawa, K. (2015). Floral colour change in the eyes of
648 pollinators: Testing possible constraints and correlated evolution. *Functional*
649 *Ecology*, 29(9), 1144–1155. <https://doi.org/10.1111/1365-2435.12420>

650 Otsu, N. (1979). A Threshold Selection Method from Gray-Level Histograms. *IEEE*
651 *Transactions on Systems, Man, and Cybernetics*, 9(1), 62–66.
652 <https://doi.org/10.1109/TSMC.1979.4310076>

653 Palma, G. R., Hackett, C. P., & Markham, C. (2023). Machine Vision Applied to
654 Entomology. In *Modelling Insect Populations in Agricultural Landscapes* (pp.
655 149–184). Cham: Springer International Publishing. [https://doi.org/10.1007/978-](https://doi.org/10.1007/978-3-031-43098-5_9)
656 [3-031-43098-5_9](https://doi.org/10.1007/978-3-031-43098-5_9)

657 Papiorek, S., Junker, R. R., Alves-dos-Santos, I., Melo, G. A. R., Amaral-Neto, L. P.,
658 Sazima, M., Wolowski, M., Freitas, L., & Lunau, K. (2016). Bees, birds and
659 yellow flowers: Pollinator-dependent convergent evolution of UV patterns. *Plant*
660 *Biology*, *18*(1), 46–55. <https://doi.org/10.1111/plb.12322>

661 Paul, N. D., & Gwynn-Jones, D. (2003). Ecological roles of solar UV radiation:
662 Towards an integrated approach. *Trends in Ecology and Evolution*, *18*(1), 48–
663 55. [https://doi.org/10.1016/S0169-5347\(02\)00014-9](https://doi.org/10.1016/S0169-5347(02)00014-9)

664 Pinna, C. S., Vilbert, M., Borensztajn, S., De Marcillac, W. D., Piron-Prunier, F.,
665 Pomerantz, A., Patel, N. H., Berthier, S., Andraud, C., Gomez, D., & Elias, M.
666 (2021). Mimicry can drive convergence in structural and light transmission
667 features of transparent wings in Lepidoptera. *ELife*, *10*, e69080.
668 <https://doi.org/10.7554/eLife.69080>

669 Prabhulinga, T., Chander, S., Arya, P. S., Bhoi, T. K., & Yele, Y. (2022). Mechanism
670 and modifications associated with mimicry and camouflage in butterfly. *Journal*
671 *of Entomological Research*, *46*(3), 667–672. [https://doi.org/10.5958/0974-](https://doi.org/10.5958/0974-4576.2022.00115.3)
672 [4576.2022.00115.3](https://doi.org/10.5958/0974-4576.2022.00115.3)

673 Prudic, K. L., Skemp, A. K., & Papaj, D. R. (2007). Aposematic coloration, luminance
674 contrast, and the benefits of conspicuousness. *Behavioral Ecology*, *18*(1), 41–
675 46. <https://doi.org/10.1093/beheco/arl046>

676 R Core Team. (2023). R Core Team 2023 R: A language and environment for
677 statistical computing. R foundation for statistical computing. [https://www.R-](https://www.R-project.org/)
678 [project.org/](https://www.R-project.org/). *R Foundation for Statistical Computing*.

679 Rasband, W. (2015). ImageJ [Software]. U. S. National Institutes of Health,
680 *Bethesda, Maryland, USA*.

681 Ronneberger, O., Fischer, P., & Brox, T. (2015). U-net: Convolutional networks for
682 biomedical image segmentation. In *Medical image computing and computer-*
683 *assisted intervention—MICCAI 2015: 18th international conference, Munich,*
684 *Germany, October 5-9, 2015, proceedings, part III 18* (pp. 234-241). Springer
685 international publishing. https://doi.org/10.1007/978-3-319-24574-4_28

686 Rother, C., Kolmogorov, V., & Blake, A. (2004). “GrabCut” - Interactive foreground
687 extraction using iterated graph cuts. *ACM Transactions on Graphics*, 23(3),
688 309–314.
689 https://doi.org/10.1145/1015706.1015720/SUPPL_FILE/PPS014.MOV

690 Shrestha, M., Dyer, A. G., Bhattarai, P., & Burd, M. (2014). Flower colour and
691 phylogeny along an altitudinal gradient in the Himalayas of Nepal. *Journal of*
692 *Ecology*, 102(1), 126–135. <https://doi.org/10.1111/1365-2745.12185>

693 Stella, D., & Kleisner, K. (2022). Visible beyond Violet: How Butterflies Manage
694 Ultraviolet. *Insects*, 13(3), 242. <https://doi.org/10.3390/insects13030242>

695 Tammaru, T., & Teder, T. (2012). Why is body size more variable in stressful
696 conditions: An analysis of a potential proximate mechanism. *Evolutionary*
697 *Ecology*, 26(6), 1421–1432. <https://doi.org/10.1007/s10682-012-9557-3>

698 van Klink, R., August, T., Bas, Y., Bodesheim, P., Bonn, A., Fossøy, F., Høye, T. T.,
699 Jongejans, E., Menz, M. H. M., Miraldo, A., Roslin, T., Roy, H. E., Ruczyński, I.,
700 Schigel, D., Schäffler, L., Sheard, J. K., Svenningsen, C., Tschan, G. F.,
701 Wäldchen, J., ... Bowler, D. E. (2022). Emerging technologies revolutionise
702 insect ecology and monitoring. *Trends in Ecology and Evolution*, 37(10), 872–
703 885. <https://doi.org/10.1016/j.tree.2022.06.001>

704 Van Rossum, G., & L. Drake, F. (2009). Python 3 Reference Manual, Scotts Valley.
705 In *Scotts Valley, CA*.

706 Watt, W. B., & Boggs, C. L. (2003). Synthesis: butterflies as model systems in
707 ecology and evolution—present and future. *Butterflies—ecology and evolution*
708 *taking flight. The University of Chicago Press, Chicago*, 603–613.

709 Wellstein, C., Schröder, B., Reineking, B., & Zimmermann, N. E. (2011).
710 Understanding species and community response to environmental change - A
711 functional trait perspective. *Agriculture, Ecosystems and Environment*, 145(1),
712 1–4. <https://doi.org/10.1016/j.agee.2011.06.024>

713 Wilson, R. J., de Siqueira, A. F., Brooks, S. J., Price, B. W., Simon, L. M., van der
714 Walt, S. J., & Fenberg, P. B. (2023). Applying computer vision to digitised
715 natural history collections for climate change research: Temperature-size
716 responses in British butterflies. *Methods in Ecology and Evolution*, 14(2), 372–
717 384. <https://doi.org/10.1111/2041-210X.13844>

718 Wood, S. N. (2023). Mixed GAM Computation Vehicle with Automatic Smoothness
719 Estimation. R package. In *Generalized Additive Models: An Introduction with R*,
720 *Second Edition*.

721 Woodward, G., Ebenman, B., Emmerson, M., Montoya, J. M., Olesen, J. M., Valido,
722 A., & Warren, P. H. (2005). Body size in ecological networks. *Trends in Ecology*
723 *and Evolution*, 20(7), 402–409. <https://doi.org/10.1016/j.tree.2005.04.005>

724 Zapletalová, L., Zapletal, M., & Konviaka, M. (2016). Habitat Impact on Ultraviolet
725 Reflectance in Moths. *Environmental Entomology*, 45(5), 1300–1305.
726 <https://doi.org/10.1093/ee/nvw097>

727

728 **SUPPORT INFORMATION**

729 **SI1.** Explanation of variables generated by LEPY

730 **SI2.** LEPY vs. ImageJ Measurement Comparison Dataset

731 **SI3.** LEPY Morphological Traits Dataset

732 **SI4.** Scale bar template